

Received 22 July 2023, accepted 27 August 2023, date of publication 6 September 2023, date of current version 13 September 2023.

Digital Object Identifier 10.1109/ACCESS.2023.3312629

APPLIED RESEARCH

Wide Band Periodic 2D Leaky-Wave Antenna for Millimeter-Wave Application

ABDULLAH ATTAR¹, (Student Member, IEEE), ISLAM AFIFI², (Member, IEEE),
AND ABDEL RAZIK SEBAK³, (Life Fellow, IEEE)

¹Department of Electrical Engineering, Taibah University, Yanbu 42353, Saudi Arabia

²Department of Engineering Mathematics and Physics, Cairo University, Cairo 12613, Egypt

³Department of Electrical and Computer Engineering, Concordia University, Montreal, QC H3G 1M8, Canada

Corresponding author: Abdullah Attar (asattar@taibahu.edu.sa)

This work was supported by Taibah University's.

ABSTRACT A wideband periodic leaky-wave antenna (LWA) is proposed in this paper. By using lossy dielectric material inside the wedge-like guide as medium for wave propagation, a leaky mode is excited and results in widening the bandwidth. For certain tangential losses, this leaky-wave antenna achieves 20.34% 3-dB gain bandwidth with maximum gain of 19.7 dBi. The antenna experiences low side lobe level (SLL) in general and low cross-polarization over the operating frequency, making the antenna suitable for millimeter-wave (mm-wave) applications.


INDEX TERMS High gain antenna, wide band antenna, millimeter-wave, leaky-wave antenna (LWA), lossy material, radial waveguide, wedge-like waveguide.

I. INTRODUCTION

The adaptation of 5G as mean of communications arises the need for uncomplicated and affordable technology. Intensive research for the new allocated band for 5G, namely the millimeter-wave (mm-wave) band, have been conducted. Since the millimeter-wave signal has high propagation loss, the majority of the antenna-related researches propose works based on substrates that have low tangential loss. These kind of substrates, although they are proper to mm-wave applications, are expensive, specially for commercial use. Comparably, much less works have investigated the possibility to design antennas using affordable substrates such as FR4, acrylonitrile butadiene styrene polycarbonate (ABS-PC), and polycarbonate substrates for mm-wave applications. Although these type of materials have higher tangential loss than the common substrates, with proper design high gain wide bandwidth antennas can be achieved.

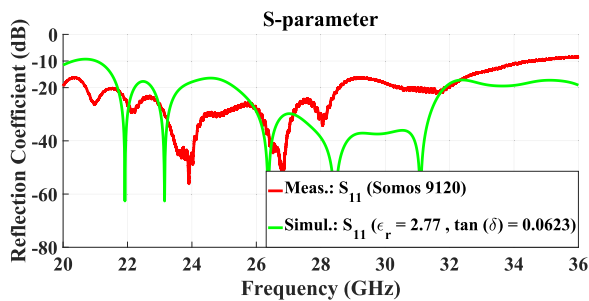
Several works have used FR4 as a substrate to design various antennas working for various frequencies [1], [2], [3], [4], [5], [6], [7]. In [1], antenna-in-package (AiP), containing

the antenna elements, its feeding line and transition, and RF interface and power, was proposed for 60 GHz at ultra low cost. Multi FR4 layers with tangential loss of 0.012 was used to form the package. The antenna exhibits 4.1 dBi gain with 76% efficiency and 15% impedance bandwidth. The antenna has moderate cross-polarization of -12 dB and suffers from high side lobe level (SLL). Patch antenna array, designed to generate mm-wave Hermite-Gaussian Beams, was introduced in [2]. This work also was directed toward mm-wave application at 73 GHz. Isola Global FR408 circuit board with 0.018 tangential loss was used as a substrate for the patch array. The array achieves 7.49 dBi gain at 56% efficiency and it gives 7.5% impedance bandwidth. Dual mm-wave band, 25.5 GHz and 76.5 GHz, monopole patches array was proposed by [3]. 0.02 tangential loss FR4 was used as a substrate for the work. The array provides 12% and 13.3% impedance bandwidth at 25.5 GHz and 76.5 GHz respectively. The works in [4] proposed multiple band using FR4 as well. A frequency-reconfigurable multi-input-multi-output (MIMO) antenna has an omni-directional gain of 1.06 dBi with 54% efficiency, 1.02 dBi with 59% efficiency, and 2.46 dBi with 73% efficiency at 2.45 GHz, 3.5 GHz, and 5.7 GHz respectively. The three respective

The associate editor coordinating the review of this manuscript and approving it for publication was Pavlos I. Lazaridis .



(a)

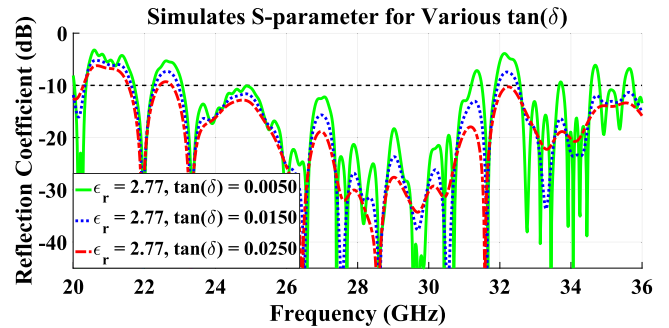


(b)

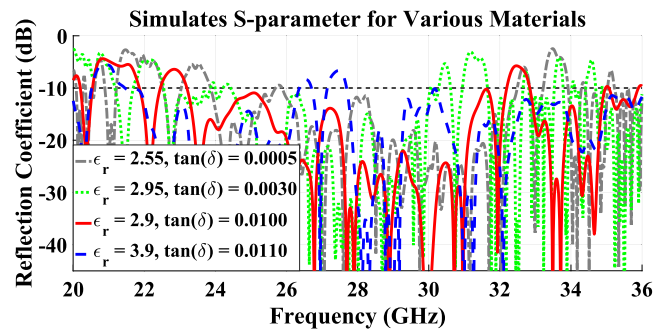
FIGURE 1. Somos 9120 Substrate. (a) 3D printed prototype. (b) Reflection coefficient for fabricated Somos 9120 substrate and the corresponding simulated substrate.

impedance bandwidths are 3.3%, 6%, and 10.5%. Both [5] and [6] proposed antennas that work at 4.5 GHz. Although both used FR4 as a substrate, the dual-polarized filtering patch antenna in [5] provides 11.11% impedance bandwidth while the reconfigurable circularly-polarized patch antenna in [6] achieves ultra-wide impedance bandwidth (UWB) of 49.28%. The efficiency for both works are 90% and more than 75%, respectively. Yet, the gain is 6 dBi for [5] and 3 dBi for [6]. Another UWB cylindrical dielectric resonator antenna with operational frequency from 3.6 GHz to 18 GHz was introduced in [7]. FR4 substrate which has 0.017 tangential loss was used and it resulted in 133% impedance and 3-dB gain bandwidths. Unlike the UWB the antenna provides, the gain is 7.9 dBi and the radiation pattern suffers from high cross-polarization and high SLL. Mateo-Segura et al. [8] have shown a case study for their proposed numerical method using FR4 as a substrate. The case study was carried through CST simulation and has shown high gain of 17 dBi with 40% radiation efficiency. The bandwidth of the simulation, however, was not reported.

As for ABS-PC, the work in [9] adopted it as substrate for their inkjet printed patch antenna. The APS-PC has tangential loss of 0.00425 at 5 GHz. This antenna has UWB of 200% (3 GHz - 13 GHz) with -20 dB cross-polarization from 3 GHz to 7 GHz. However, the cross-polarization becomes severely high from 7 GHz to 13 GHz. The gain of this antenna is 4.2 dBi. Both [10] and [11] used ABS-PC



(a)



(b)

FIGURE 2. Parametric Study for S_{11} . (a) Various losses for the same relative permittivity of 2.77. (b) Various dielectric materials. Namely: Preperm 255, Arlon Ad 295, Polycarbonate, and Getek ML200C, respectively.

material as well but without achieving considerable BW as the reflection coefficient failed to be lower than -6 dB over the intended operational band.

Polycarbonate was used in several works such as [12], [13], [14], [15], [16], [17], [18], and [19]. Performance analysis was conducted by [13] at 2.535 GHz using polycarbonate substrate. The fabricated microstrip patch antenna achieves 4.4 dBi directivity and 3.8 dBi gain, resulting in 87% radiation efficiency. The impedance bandwidth of this antenna is 17.5%. Bowtie dipole was designed by [14] adopting 0.008 tangential loss polycarbonate material as a substrate. By tapering the bowtie, the antenna provides 1.67 dBi gain for 8.6% impedance bandwidth. Polycarbonate was also used by [15] in designing compact antipodal Vivaldi antenna. The antenna has moderate gain of 12.7 dBi at 28 GHz. However, it suffers from high SLL. The reported impedance bandwidth is 240%, ignoring the instability of the radiation pattern over this bandwidth. In [16], dual-polarized microstrip patch array antenna was presented. 6.5 dBi gain, 77% radiation efficiency, and 5.3% impedance bandwidth have been achieved when Lexan substrate was used. The cross-polarization is less than -15 dB. On the contrary, the array has high SLL. Yet another antipodal Vivaldi antenna with polycarbonate substrate ($\tan(\theta) = 0.01$) was proposed in [17]. This antenna was addressed toward mm-wave 5G applications (center frequency is 28 GHz) and has wide impedance bandwidth of 35%. However, its gain is moderate (10 dBi) and its

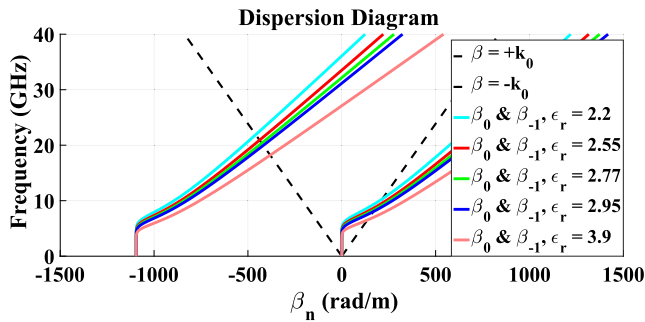


FIGURE 3. β -diagram for different dielectric materials. Namely: RogersRogers RT 5880 (2.2), Preperm 255 (2.55), Somos 9120 (2.77), polycarbonate (2.95), and Getek ML200C (3.9).

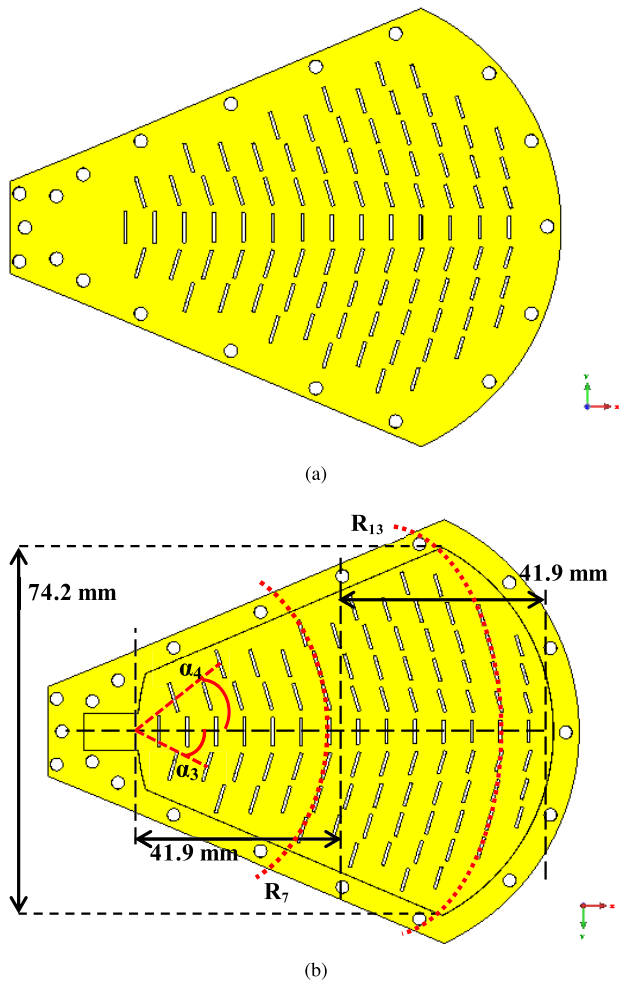


FIGURE 4. Layout for the proposed antenna with polycarbonate substrate. (a) Top view. (b) Bottom view.

SLL is high (-5 dB). Reference [18] targeted mm-wave 5G devices as well through designing polycarbonate-based flexible antenna. The designed antenna has 7 dBi gain, 16.1% impedance bandwidth, and -8 dB SLL. 11.71 dBi gain has been achieved by [19] with 70.8% efficiency over 9.7% impedance bandwidth for their polycarbonate-based on-chip antenna which works at 0.3 THz. The antenna experiences

TABLE 1. Slots details for each ring (all slots have width of 0.6 mm).

Ring	Radius (mm)	Slot Length (mm)	α (degree)
1	4.2946 (0.637 λ_g)	6.264	—
2	10.0325 (1.488 λ_g)	6.123	44.4
3	15.7703 (2.339 λ_g)	5.982	27.56
4	21.5082 (3.19 λ_g)	5.841	19.78
5	27.2461 (4.041 λ_g)	5.701	15.3
6	32.984 (4.892 λ_g)	5.56	12.37
7	38.7218 (5.743 λ_g)	5.418	10.3
8	44.4597 (6.594 λ_g)	5.136	8.6
9	50.1976 (7.446 λ_g)	4.995	7.47
10	55.9354 (8.297 λ_g)	4.854	6.56
11	61.6733 (9.148 λ_g)	4.713	5.8
12	67.4112 (9.999 λ_g)	4.572	5.2
13	73.1491 (10.85 λ_g)	4.431	4.68
14	78.8869 (11.701 λ_g)	4.29	4.24

very low SLL which is understandable considering the enormous electrical size of the antenna.

Several other works tried various lossy substrate as in [20], [21], [22], and [23]. Reference [20] used PCB with 0.023 tangential loss, [21] used resin-coated photo paper with 0.05 tangential loss, [22] adopted Taconic Substrate with 0.006 tangential loss, and [23] used Kapton substrate with 0.007 tangential loss. The achieved bandwidths are 3.33%, 47%, 1.6%, and 119%, respectively. The gains for the last three works are 3 dBi, 6.65 dBi, and 5.5 dBi, respectively.

In all these works, either wide bandwidth has been achieved with low and moderate gain, or high gain has been provided over moderate bandwidth. For mm-wave applications, both gain and bandwidth are to be maximized to utilize the potential of the mm-wave spectrum. In addition, the radiation pattern should have acceptable characteristics in terms of SLL, cross-polarization, and stability of the radiation shape itself. The low cost has to be maintained as well. Accordingly, this work presents a novel utilization of polycarbonate material that satisfies these traits. By using this lossy material as substrate, high gain wide band leaky-wave antenna is proposed. The antenna experiences low SLL and cross-polarization over its band. Section II of this paper addresses the background of the work. Section III shows the design of the antenna, Section IV presents the simulation results, Section V verify the work through fabricated prototype and measurements, Section VI discusses the comparison between this work and other related works, and Section VII concludes the paper.

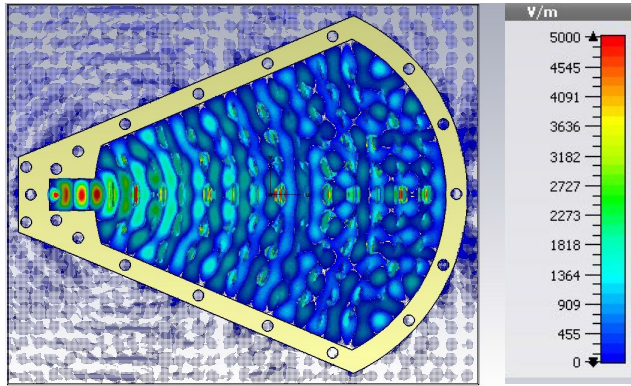


FIGURE 5. E-field distribution inside the wedge-like waveguide at 26.5 GHz.

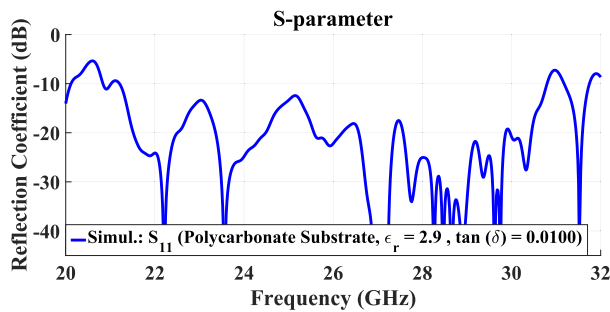


FIGURE 6. Simulated reflection coefficient for the proposed antenna.

II. SELECTION OF MATERIAL

As a mean of adopting 3D printing technology for the fabrication process, Somos 9120, a polypropylene-like material [24], was initially used to print the substrate of [25]. Somos 9120 substrate had very good reflection coefficient although it was not matching the simulation results.

The radiation patterns, on the other hand, were very poor in terms of the gain despite their resemblance to the simulated patterns. After examining the polypropylene-like material through free space method at 33 GHz, Somos 9120 material was found to be a lossy one with relative permittivity of 2.77 and tangential loss of 0.0623. Using CST, the design of [25] was used with a customized substrate of similar characteristics (2.77 permittivity and 0.0623 tangential loss) to simulate and confirm the results of the measured radiation pattern. Figure 1 shows the printed Somos 9120 substrate along with the resulted reflection coefficients.

This reflection coefficient has good matching over the operational and non-operational bandwidth. The simulated radiation patterns behave the same at 33 GHz with a small shift of 0.5°. However, for other frequencies, there are differences in the gain's amplitudes. This can be justified by the tangential loss sensitivity to the change of frequency for this material. As the frequency increases, the losses increases as well for Somos 9120 material. The material undergoes changes in the relative permittivity as well. That is, the relative permittivity increases as the frequency increases.

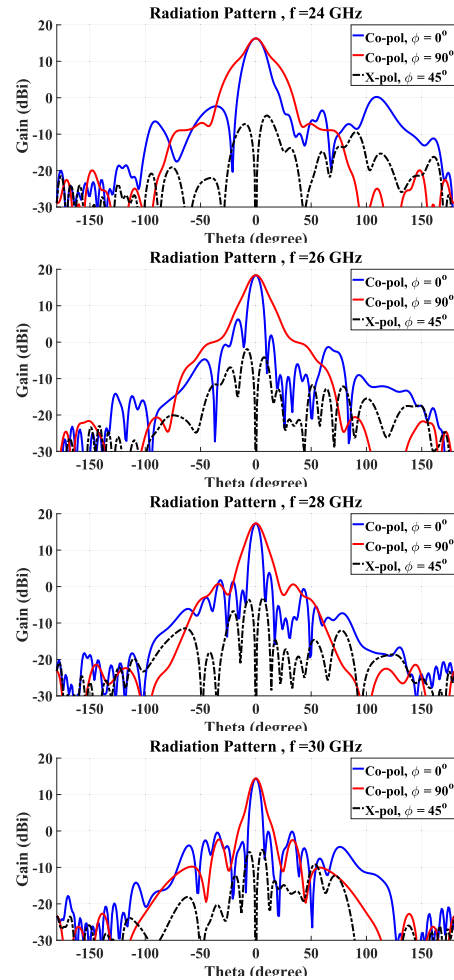


FIGURE 7. Simulated radiation patterns for polycarbonate substrate ($\epsilon_r = 2.9$ and $\tan(\delta) = 0.01$) at various frequencies.

Henceforth, by using material with relative permittivity that lays between 2.8 and 3.0 but with lower tangential loss (between 0.005 and 0.01), it is possible to expand the operational bandwidth while minimizing the drop in the gain.

Running the simulation of this antenna while matching the relative permittivity, reducing the losses potentially, and maintaining the original antenna's dimensions has shown extremely bad performance where no acceptable radiation pattern is observed. This shows that the key factor here is the losses themselves. The reason is that the propagated wave has weakened as it moves through the lossy material. Accordingly, by the end of the waveguide, the wave is very weak and its reflection does not disturb both the inner forward waves and the outer radiated waves. Various tangential loss values were simulated. Considering relative permittivity of 2.77, the proper value to achieve good reflection coefficient performance lays between 0.005 and 0.015. However, since no material has the desired tangential loss that corresponds to 2.77 permittivity, various materials were tested to find the nearest acceptable permittivity with its corresponding tangential loss. The parametric study for the reflection coefficient is shown in Figure 2.

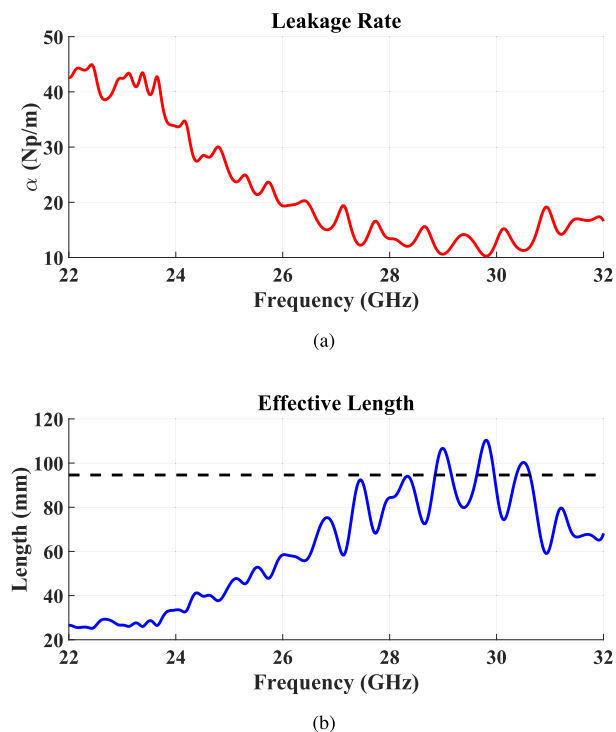


FIGURE 8. Leakage rate and corresponding effective length. (a) Leakage Rate α for the operational bandwidth. (b) Effective length corresponding to each α . Effective length is calculated by considering that 90% of the power is leaked. The black dotted line shows the total length of the antenna (83.8 mm).

With the original design of [25] and based on its analytical part, polycarbonate ($\epsilon_r = 2.9$ and $\tan(\delta) = 0.01$) shows good reflection coefficient performance, covering the band from 22 GHz to 33 GHz. Henceforth, polycarbonate material is adopted as the new substrate for the antenna.

III. ANTENNA DESIGN

When using polycarbonate material as a substrate, [25] design shows good impedance bandwidth and acceptable radiation pattern as mentioned earlier. However, the slots lengths do not account for the new operational frequency. The beta diagram, Figure 3, for the polycarbonate material (ϵ_r) shows operational bandwidth starting above 20 GHz, which corresponds to 65° beam tilt, and reaches the broadside at 31 GHz.

Accordingly, the antenna is redesigned, in terms of slots length and distribution along each ring, while maintaining the antenna's wedge-like waveguide, thickness, and feeding. The layout of the new design is shown in Figure 4. To begin with, the polycarbonate-filled wedge-like waveguide is adopted for the wave to propagate within. The height of this waveguide (2.54 mm) is chosen to support the quasi-TEM mode since it is less than $\lambda_g/2$. The dielectric functions as slower surface to slow the wave propagation in the frequency range of interest where all harmonics are in slow-wave zone, to prevent the radiation in that range, except for β_{-1} harmonic which is in

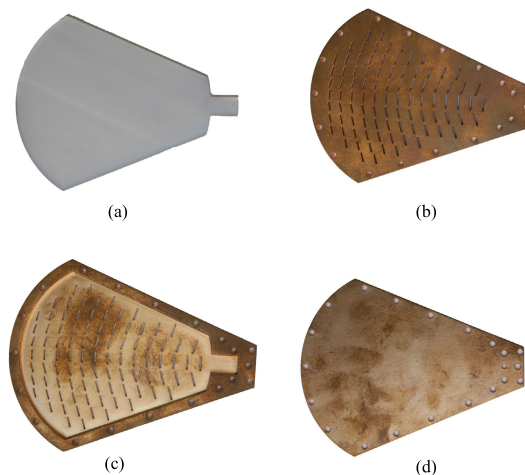


FIGURE 9. (a) Lexan Material used as substrate. (b) Prototype antenna (top view). (c) Prototype Shell with Lexan material inside (bottom view). (d) Ground sheet.

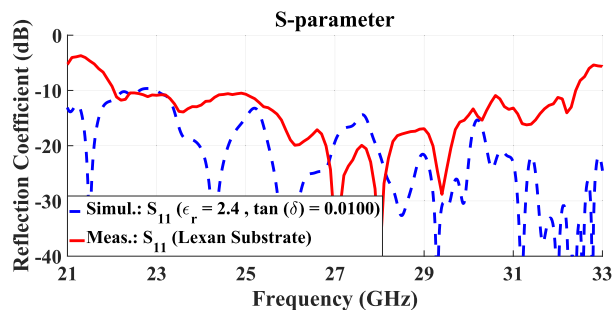


FIGURE 10. Simulated reflection coefficient for the proposed antenna.

fast-wave zone. A back short-terminated polycarbonate-filled rectangular waveguide feeds the wedge-like waveguide from the narrow end of the wedge. The rectangular waveguide is excited by a probe of 1.6855 mm ($\lambda_g/4$) length placed $\lambda_g/4$ from the short-terminated back of the rectangular waveguide. The flaring angle of the wedge-like waveguide is 67° and it is chosen based on E-field propagated inside the guide as shown in Figure 5, imitating the wave as it propagates. Fourteen rings of slots are placed on the top surface of the wedge-like waveguide to radiate the power. The actual spacing between the rings is chosen based on the strength of the field as the wave propagates. The slots lengths are designed to cover the operational bandwidth in which the longer slots at the first rings resonate with lower limit of the band whereas the shorter slots at the last rings resonate with the upper limit of the band. This is due to property of leaky-wave antenna in which the slots' excitation is of progressive nature. That is, not all slots are excited at the same time/phase. Rather, each ring with its slots is excited as the wave propagates from the the probe of the antenna to the front. Also, the slots are tilted away from the y-axis to improve SLL. Finally, the gaps between the slots within the same ring (α) are spaced to maximize the slots' number in

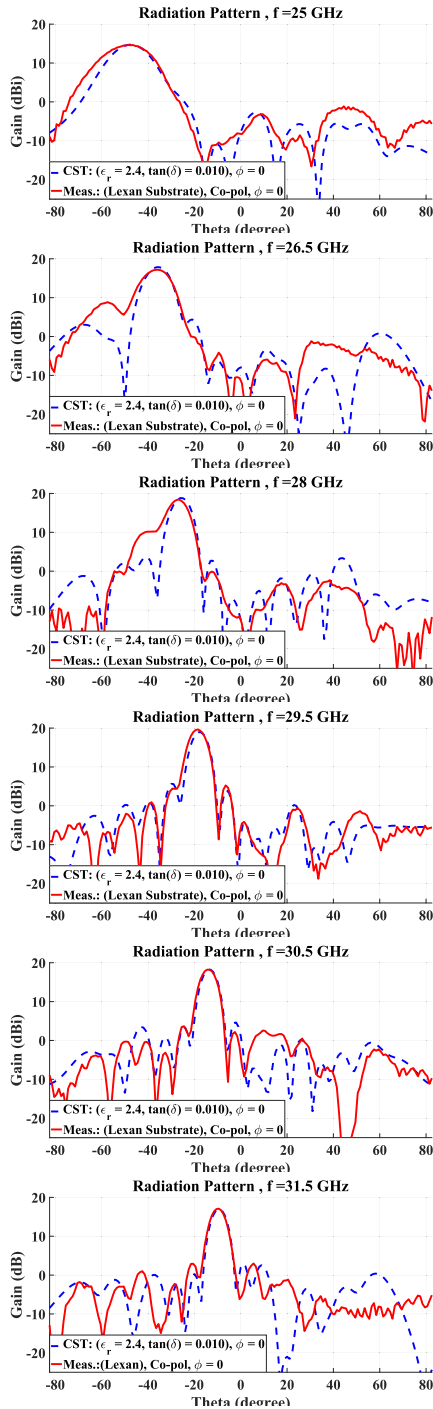


FIGURE 11. Simulated and measured radiation patterns for modified substrate ($\epsilon_r = 2.4$ and $\tan(\delta) = 0.01$) and Lexan substrate, respectively, for various frequencies.

order to capture the field. The optimized dimensions of the proposed antenna are shown in Table 1.

IV. SIMULATION RESULTS

Using CST STUDIO package to perform full wave analysis, the simulation shows good performance in terms of reflection coefficient, achieved gain and radiation patterns, sidelobe levels (SLL) and cross-polarization. Figure 6 shows

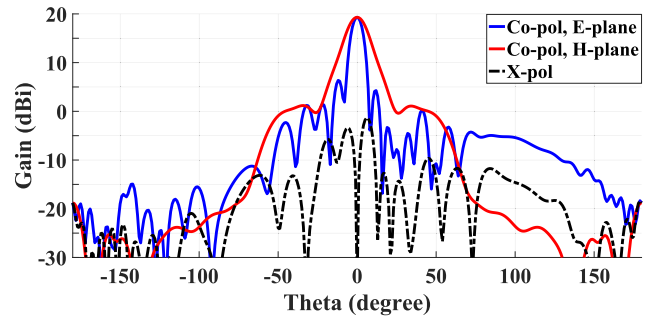


FIGURE 12. Normal alignment for E and H plane beams at 29.5 GHz.

the reflection coefficient of this new design. The achieved simulated impedance bandwidth is 36.2%, starting from 21.2 GHz up to 30.8 GHz. The radiation pattern, shown in Figure 7, over the operational bandwidth has maximum gain of 18.45 dBi at 26.5 GHz, average SLL of -14.6 dB for $0^\circ\phi$ -cut, average SLL of -25.6 dB for $90^\circ\phi$ -cut, and average cross-polarization of -22 dB.

Since the proposed antenna is symmetrical around the propagation axis, the H-plane (corresponding to $90^\circ\phi$ -cut) shows symmetrical radiation pattern. Moreover, since the slots are arranged in curvilinear fashion to imitate a wavefront-shape, the resulted SLL is very low since the propagated wave reaches each ring with the same phase. The E-plane (corresponding to $0^\circ\phi$ -cut), on the other hand, experience asymmetrical formation for the rings where the rings differ with each other in both the number of the slots and their lengths. In addition, the slots' excitation is of progressive nature. That is, The rings/slots are excited progressively as the wave propagates from the back to the front and they do not experience the excitation at the same time nor they experience the same excitation phase, as mentioned previously. Thusly, the radiation pattern is asymmetrical in E-plane as well. For the average SLL of E-plane (-14.6 dB), the lowest SLL (-19.6 dB) occurs at 23 GHz while the highest one (-11.7 dB) occurs at 27 GHz. For the average SLL of H-plane (-25.6 dB), on the other hand, the lowest SLL is 44.7 dB at 27.5 GHz whereas the highest SLL is -12.9 at 30.5 GHz. As for the cross-polarization, the values over the operational band oscillate between -20.3 dB and -24.1 . The orientation of the slots with respect to y-axis contributes heavily on the cross-polarization value. More slot's tilt-away from the y-axis would result in lower cross-polarization and vice versa. As mentioned earlier, slots are tilted away from y-axis to improve SLL on the account of cross-polarization. Nevertheless, the values of cross-polarization are still low.

Unlike the case in [25], where the α is the main contributor to radiated power, the radiated power of this proposed antenna is heavily affected by material loss along with α . This affects the radiation efficiency considerably. The radiation efficiency starts from 67% but drops to 10% as the frequency increases. The seemingly low efficiency, in general, is due to the nature of propagation inside the wedge-like waveguide. Since the propagated wave is propagating within two dimensions, it is

TABLE 2. Comparison between lossy-substrate based antennas.

Ref.	Substrat Material	$\tan(\delta)$	Freq. (GHz)	Gain (dBi)	SLL (dB)	Grating/Back Lobe (dB)	x-pol. (dB)	Imped. BW (%)	3-dB Gain BW (%)	Area (λ_0^2)
[1]	FR4	0.012	60	4.1	-4	-4	-12	15	15	2.16 ($1.8\lambda_0 \times 1.2\lambda_0$)
[2]	FR4	0.018	73	7.49	-12	N/R	N/R	7.5	N/R	3.77 ($1.9\lambda_0 \times 1.9\lambda_0$)
[4]	FR4	N/R	5.7	2.46	N/R	-5	-15	10.5	N/R	0.43 ($1.14\lambda_0 \times 0.38\lambda_0$)
[17]	Polycarbonate	0.01	28	9.8	-5	-17	N/R	39.3	39.3	6.1 ($3.3\lambda_0 \times 1.87\lambda_0$)
[18]	Polycarbonate	0.01	28	7	-8	-18	N/R	16.5	16.5	9 ($3\lambda_0 \times 3\lambda_0$)
[19]	Polycarbonate	0.01	300	11.71	-30	-30	N/R	9.7	9.7	7×10^7 ($20000\lambda_0 \times 3500\lambda_0$)
[21]	Photo Paper	0.05	5	3	N/A	N/A	< -10	47	N/R	0.39 ($0.58\lambda_0 \times 0.67\lambda_0$)
[22]	Taconic	0.006	1.268	6.65	-17	-21.9	-27	1.6	N/R	0.44 ($0.51\lambda_0 \times 0.87\lambda_0$)
This Work	Polycarbonate	0.01	28.5	19.7	-13.1	-24.5	-20.6	33.9	20.34	40.7

TABLE 3. Comparison between various types of leaky-wave antennas covering K_a band.

Ref.	Substrat Material	$\tan(\delta)$	Freq. (GHz)	Gain (dBi)	SLL (dB)	Grating/Back Lobe (dB)	x-pol. (dB)	Imped. BW (%)	3-dB Gain BW (%)	Area (λ_0^2)	Scanning Range (degree)
[27]	Air	0	29	18.5	-12	-15.5	N/R	22	10.34	33 ($7.77\lambda_0 \times 4.25\lambda_0$)	17
[28]	Air	0	28.5	24	-15	-16	-75	7	7	816 ($192\lambda_0 \times 4.25\lambda_0$)	9
[29]	Air	0	26.5	14.2	-3	-13	-15	18.9	7.6	27.6 ($7.1\lambda_0 \times 3.89\lambda_0$)	10
[30]	RT5880	0.0009	28	16.6	-12	No Lobe	-24.1	17.9	17.9	9.2 ($7.9\lambda_0 \times 1.3\lambda_0$)	17
[31]	RO3006	0.002	26.5	12.2	-12	No Lobe	-20	41.5	17	14 ($8\lambda_0 \times 1.75\lambda_0$)	45
[32]	RO4350B	0.0037	31	14	-15	-10	-12	29	29	17 ($11.4\lambda_0 \times 1.5\lambda_0$)	70
[33]	Air	0	38	19.5	-20	-25	-50	15.8	15.8	76 ($76\lambda_0 \times 1\lambda_0$)	51
[34]	RT6002	0.0012	36	10.5	-5	-16	N/R	11	3	5.2 ($8.4\lambda_0 \times 0.62\lambda_0$)	49
[35]	RO4003	0.0027	26	16.5	-15	-30	N/R	23	23	4.1 ($13.6\lambda_0 \times 0.3\lambda_0$)	37
[36]	Taconic TLY-5-0200	0.0009	29.25	16.2	-13	N/R	N/R	25	18	33 ($151\lambda_0 \times 2.2\lambda_0$)	59
[25]	RT5880	0.0009	32	20.34	-13	-14.7	-28.6	24.4	15	30	44
This Work	Polycarbonate	0.01	28.5	19.7	-13.1	-24.5	-20.6	33.9	20.34	40.7	62

TABLE 4. Comparison between 2D leaky-wave antennas.

Ref.	Substrat Material	$\tan(\delta)$	Freq. (GHz)	Gain (dBi)	SLL (dB)	Grating/Back Lobe (dB)	x-pol. (dB)	Imped. BW (%)	3-dB Gain BW (%)	Area (λ_0^2)	Scanning Range (degree)
[37]	($\epsilon_r = 10.2$)	0.0023	19.48	18.55	-10	N/R	-10	20.5	5.1	43.6 ($6.6\lambda_0 \times 6.6\lambda_0$)	17
[38]	Taconic TLY5	0.0009	18	N/R	-5	-22	N/R	40	N/R	221	N/R
[39]	Air	0	237.5	28.5	-10.9	-10	N/R	6.3	6.3	238.5 ($35.6\lambda_0 \times 6.7\lambda_0$)	50
[40]	Air	0	42	29.2	-14	N/R	N/R	38	23.8	241.8 ($18.6\lambda_0 \times 13\lambda_0$)	54
[41]	RT6010	0.0023	10.1	23	-14.4	N/R	N/R	14.85	14.85	69.6 ($8\lambda_0 \times 8.7\lambda_0$)	62
This Work	Polycarbonate	0.01	28.5	19.7	-13.1	-24.5	-20.6	33.9	20.34	40.7	62

exposed to more lossy area than if it propagates in one dimension only. As the frequency increases, the wavelength gets shorter and the propagating distance increases, resulting

in more lossy dielectric areas to be penetrated. Low efficiency due to 2 dimensional propagation has been the case too for the case study conducted by [8].

The leakage rate of the proposed antenna is shown in Figure 8 (a). The antenna experiences high leakage rate at the lower band of the operational frequency which means that most of the power is radiated through the early rings. This rate drops for the higher band of the operational bandwidth as more rings participate in radiating the power. This is noticeable from Figure 8 (b) which shows the effective length of the proposed antenna. At 24.5 GHz, for instance, 90% of the power is radiated mostly through half of the rings while at 28 GHz the same amount of power approximately is radiating utilizing mostly all rings of the antenna. This in part explains the higher gain at these frequencies when compared to the lower ones. That is, as the power is radiated through more rings, larger area of the aperture is utilized and, henceforth, the gain increases. The effective length figure shows that the length needed to radiate 90% of the power exceeds the physical length of the antenna for the frequencies 29 GHz, 30 GHz and 30.5 GHz. Practically, this means that less than 90% of the power has been radiated. With the used physical length, approximately 80% of power is radiated at 29 GHz, 75% of power is radiated at 30 GHz, and 85% of power is radiated at 30.5 GHz.

V. FABRICATION AND MEASUREMENTS

A prototype of the proposed antenna has been manufactured. Two methods are involved in fabricating the prototype. First, CNC machining is used to fabricate the substrate. Transparent Lexan sheet, a polycarbonate material, is used as the substrate. This material has 0.001 dissipation factor at 50-60 Hz and 0.01 at 1 MHz. The dielectric constant for this material drops from 3.17 at 50-60 Hz to 2.98 at 1 MHz [26]. Second, 3D printing technology, mainly Stereolithography, is used to print the outer body of the antenna. Plastic material is printed first and then plated by copper of 0.002" (0.0508 mm) thickness. Semi-bright finishing is used to smooth both the inside and the outside surfaces of the outer body. The bottom piece is printed and plated separately to be attached with the outer body through plastic screws after inserting the Lexan substrate inside the outer body. Figure 9 shows the prototype and its disassembled parts.

Initially, the prototype showed good impedance matching where it was below -10 dB from 22 GHz to 32 GHz, making an impedance bandwidth of 33.9%. However, there was a shift between the measured and simulated S_{11} . This shift affected the radiation pattern and created a mismatch between the simulated and measured results. The cause of the shift is the change of relative permittivity at higher frequencies. Apparently, the value becomes lower at K and K_a bands. The ϵ_r at those bands is roughly around 2.4. Accordingly, re-simulation of the performance is conducted using the new ϵ_r of 2.4. The new simulated results are in good match with the measured ones. Figure 10 shows the reflection coefficient of both the simulated and measured results while Figure 11 shows the radiation patterns of E-planes. The maximum achieved gain is 19.7 dBi occurring at 29.5 GHz. The proposed antenna has average gain of 16.7 dBi and average SLL

of -13.1 dB and able to scan from -62° to -1° . In addition, the 3-dB gain bandwidth is 20.34%. The co-polarization radiation patterns for E-plane and H-plane along with the respective cross-polarization at 29.5 GHz are shown in Figure 12.

VI. DISCUSSION

Comparison between the proposed antenna and other various antennas are shown in the following tables. In Table 2, the proposed antenna is compared with various type of antennas that used similar substrate material. It is clear from the table that this work surpasses all of these works in the achieved gain. In addition, it has a low SLL compare to the presented works except for [19] (which has very long electrical length with respect to its operational frequency) and [22] (which provides omni-directional radiation).

In the next table, 1D LWAs designed for K_a band are considered only. This is to compare the antennas addressed to the same type of applications, namely millimeter-wave applications. The proposed antenna shows good performance for a high gain antenna. It surpasses other works with higher gain ([25], [28], and [33]) in terms of both impedance bandwidth and 3-dB gain bandwidth. Although [32] and [35] have higher 3-dB gain bandwidth, both works provide moderate gain. Moreover, the proposed antenna has the second widest scanning range.

Table 4 shows the comparison between the proposed work and the other 2D LWAs. The comparison is set separately since these antennas operate in different bands. This work achieves the widest scanning range along with [41], the lowest back-lobe and cross-polarization, and the second widest impedance bandwidth and 3-dB gain bandwidth. The noticeable higher gain achieved by other works is due to the very big electrical length of these works, which makes this work the most compact work in terms of size among the other 2D LWAs. Regardless, the proposed antenna performs well in all aspects when compared to other antennas.

VII. CONCLUSION

The utilization of low-cost polycarbonate in achieving high gain wide bandwidth antenna has been proven. The usage of Somos 9120 lossy material led to new design. First, the idea was validated through CST simulation. Then material investigation was conducted. Proper material (polycarbonate) was chosen to be the substrate and the final design was simulated and validated using this material. Practically, Lexan material, a polycarbonate material was adopted. The Lexan's relative permittivity tends to get low as the frequency increases. The tangential loss variation, on the other hand, seems to be less significant (around 0.01) for the operational bandwidth. The fabrication of the antenna was done through CNC machining for the Lexan part and Stereolithography 3D printing for the outer shell. Good performance has been achieved in terms of maximum gain (19.7 dBi), impedance bandwidth (33.9%), and SLL (-13.1 dB on average). The simulation and measured results match each other greatly.

ACKNOWLEDGMENT

The authors would like to thank Riddhi Goswami and Dr. Ahmed Kishk for helping with the free space method to measure the permittivity of Somos 9120 material, and also would like to thank Mohammad Abdullah Hussini for helping with reflection coefficient measurement.

REFERENCES

- [1] W. Hong, K.-H. Baek, and A. Goudelev, "Multilayer antenna package for IEEE 802.11ad employing ultralow-cost FR4," *IEEE Trans. Antennas Propag.*, vol. 60, no. 12, pp. 5932–5938, Dec. 2012.
- [2] H. Yao, H. Kumar, T. Ei, N. Ashrafi, S. Ashrafi, D. L. MacFarlane, and R. Henderson, "Patch antenna array for the generation of millimeter-wave Hermite–Gaussian beams," *IEEE Antennas Wireless Propag. Lett.*, vol. 15, pp. 1947–1950, 2016.
- [3] M. I. Ibrahim, M. G. Ahmed, M. El-Nozahi, A. M. E. Safwat, and H. El-Hennawy, "Design and performance analysis of a miniature, dual-frequency, millimeter wave linear phased array antenna," *IEEE Trans. Antennas Propag.*, vol. 65, no. 12, pp. 7029–7037, Dec. 2017.
- [4] S. Pandit, A. Mohan, and P. Ray, "Compact frequency-reconfigurable MIMO antenna for microwave sensing applications in WLAN and Wimax frequency bands," *IEEE Sensors Lett.*, vol. 2, no. 2, pp. 1–4, Jun. 2018.
- [5] Y. Zhang, Y. Zhang, D. Li, Z. Niu, and Y. Fan, "Dual-polarized low-profile filtering patch antenna without extra circuit," *IEEE Access*, vol. 7, pp. 106011–106018, 2019.
- [6] T. Jhajharia, V. Tiwari, and D. Bhatnagar, "Polarisation reconfigurable dual-band circularly polarised patch antenna with defected ground plane for C-band wireless applications," *IET Microw., Antennas Propag.*, vol. 13, no. 14, pp. 2551–2558, 2019.
- [7] C. Zebiri, D. Sayad, I. T. E. Elfergani, J. S. Kosha, W. F. A. Mshwat, C. H. See, M. Lashab, J. Rodriguez, K. H. Sayidmarie, H. A. Obeidat, and R. A. Abd-Alhameed, "Antenna for ultra-wideband applications with non-uniform defected ground plane and offset aperture-coupled cylindrical dielectric resonators," *IEEE Access*, vol. 7, pp. 166776–166787, 2019.
- [8] C. Mateo-Segura, G. Goussetis, and A. P. Feresidis, "Sub-wavelength profile 2-D leaky-wave antennas with two periodic layers," *IEEE Trans. Antennas Propag.*, vol. 59, no. 2, pp. 416–424, Feb. 2011.
- [9] D. Unnikrishnan, D. Kaddour, S. Tedjini, E. Bihar, and M. Saadaoui, "CPW-fed inkjet printed UWB antenna on ABS-PC for integration in molded interconnect devices technology," *IEEE Antennas Wireless Propag. Lett.*, vol. 14, pp. 1125–1128, 2015.
- [10] T. Van Trinh, G. Kim, J. Kim, and C. Won Jung, "Wideband internal PIFA-loop antenna designed on the bezel of digital television applications for UHF band," *Electron. Lett.*, vol. 54, no. 22, pp. 1260–1262, Nov. 2018.
- [11] T. Van Trinh and C. W. Jung, "Compact broadband internal monopole antenna with parasitic strips and sleeve feed for UHD-TV applications," *IET Microw., Antennas Propag.*, vol. 13, no. 12, pp. 2096–2101, Oct. 2019.
- [12] A. Fantì, R. Secci, G. Boi, S. Casu, G. A. Casula, G. Mazzarella, and G. Montisci, "A polycarbonate RFID tag for blood chain tracking," in *Proc. IEEE Int. Symp. Antennas Propag. USNC/URSI Nat. Radio Sci. Meeting*, Jul. 2015, pp. 356–357.
- [13] A. Kaur, A. S. Dhillon, and E. Sidhu, "Performance analysis of microstrip patch antenna employing acrylic, Teflon and polycarbonate as low dielectric constant substrate materials," in *Proc. Int. Conf. Wireless Commun., Signal Process. Netw. (WiSPNET)*, Mar. 2016, pp. 2090–2093.
- [14] N. M. Nadzir, M. K. A. Rahim, N. A. Samsuri, F. Zubir, O. Ayop, and H. A. Majid, "UHF RFID tag using polycarbonate material," in *Proc. IEEE Asia-Pacific Conf. Antennas Propag. (APCAP)*, Aug. 2018, pp. 530–531.
- [15] N. Verma, P. Dalal, and P. Nijhawan, "Design of compact antipodal Vivaldi antenna on 250 μm and 500 μm polycarbonate over wide frequency range," in *Proc. 6th Int. Conf. Signal Process. Integr. Netw. (SPIN)*, 2019, pp. 885–890.
- [16] J. L. Kubwimana, N. J. Kirsch, C. Ziegler, G. Kontopidis, and B. Tuner, "Dual-polarized 5.75 GHz optically transparent antenna arrays," *IEEE Antennas Wireless Propag. Lett.*, vol. 18, no. 7, pp. 1512–1516, Jul. 2019.
- [17] D. Santhoshi, G. Shivani, D. R. Krishna, and S. K. Koul, "Dielectric loaded polycarbonate based antipodal Vivaldi antenna for mmWave 5G applications," in *Proc. IEEE Indian Conf. Antennas Propagation (InCAP)*, Dec. 2019, pp. 1–4.
- [18] S. K. Koul and G. S. Karthikeya, "Polycarbonate based flexible antennas for mmWave 5G devices," in *Proc. IEEE Asia-Pacific Microw. Conf. (APMC)*, Dec. 2019, pp. 28–30.
- [19] M. Alibakhshikenari, B. S. Virdee, M. Khalily, C. H. See, R. Abd-Alhameed, F. Falcone, T. A. Denidni, and E. Limiti, "High-gain on-chip antenna design on silicon layer with aperture excitation for terahertz applications," *IEEE Antennas Wireless Propag. Lett.*, vol. 19, no. 9, pp. 1576–1580, Sep. 2020.
- [20] Y. G. Kim and W. Hong, "Radiation efficiency-improvement using a via-less, planar ZOR antenna for wireless ECG sensors on a lossy medium," *IEEE Antennas Wireless Propag. Lett.*, vol. 13, pp. 1211–1214, 2014.
- [21] H. F. Abutarboush, M. F. Farooqui, and A. Shamim, "Inkjet-printed wide-band antenna on resin-coated paper substrate for curved wireless devices," *IEEE Antennas Wireless Propag. Lett.*, vol. 15, pp. 20–23, 2016.
- [22] D. Gao, Z.-X. Cao, S.-D. Fu, X. Quan, and P. Chen, "A novel slot-array defected ground structure for decoupling microstrip antenna array," *IEEE Trans. Antennas Propag.*, vol. 68, no. 10, pp. 7027–7038, Oct. 2020.
- [23] H. F. Abutarboush, W. Li, and A. Shamim, "Flexible-screen-printed antenna with enhanced bandwidth by employing defected ground structure," *IEEE Antennas Wireless Propag. Lett.*, vol. 19, no. 10, pp. 1803–1807, Oct. 2020.
- [24] MatWeb. *Overview of Materials for Polypropylene, Molded*. [Online]. Available: <http://www.matweb.com/search/DataSheet.aspx?MatGUID=08fb0f47ef7e454fbf7092517b2264b2>
- [25] A. Attar and A. R. Sebak, "High gain periodic 2-D leaky-wave antenna with backward radiation for millimeter-wave band," *IEEE Open J. Antennas Propag.*, vol. 2, pp. 49–61, 2021.
- [26] Complex Plastics Inc. (Dec. 2, 2011). *Typical Physical Properties LEXAN/MARLEX/IMPLEX/MARLON/POLYCARBONATE*. [Online]. Available: <http://www.complexplastics.com/chartlex.htm>
- [27] M. A. Sharkawy and A. A. Kishk, "Long slots array antenna based on ridge gap waveguide technology," *IEEE Trans. Antennas Propag.*, vol. 62, no. 10, pp. 5399–5403, Oct. 2014.
- [28] M. Al Sharkawy, A. Foroozesh, A. A. Kishk, and R. Paknys, "A robust horn ridge gap waveguide launcher for metal strip grating leaky wave antenna," *IEEE Trans. Antennas Propag.*, vol. 62, no. 12, pp. 6019–6026, Dec. 2014.
- [29] M. Al Sharkawy and A. A. Kishk, "Split slots array for grating lobe suppression in ridge gap guide," *IEEE Antennas Wireless Propag. Lett.*, vol. 15, pp. 946–949, 2016.
- [30] K.-M. Mak, K.-K. So, H.-W. Lai, and K.-M. Luk, "A magnetoelectric dipole leaky-wave antenna for millimeter-wave application," *IEEE Trans. Antennas Propag.*, vol. 65, no. 12, pp. 6395–6402, Dec. 2017.
- [31] M. H. Rahmani and D. Deslandes, "Backward to forward scanning periodic leaky-wave antenna with wide scanning range," *IEEE Trans. Antennas Propag.*, vol. 65, no. 7, pp. 3326–3335, Jul. 2017.
- [32] D. Cao, Y. Li, and J. Wang, "Spoof surface plasmon polaritons fed frequency-scanning open-loop antenna arrays," *IEEE Access*, vol. 7, pp. 179954–179960, 2019.
- [33] Q. Yang, X. Zhao, and Y. Zhang, "Design of CRLH leaky-wave antenna with low sidelobe level," *IEEE Access*, vol. 7, pp. 178224–178234, 2019.
- [34] D. Zheng, Y.-L. Lyu, and K. Wu, "Transversely slotted SIW leaky-wave antenna featuring rapid beam-scanning for millimeter-wave applications," *IEEE Trans. Antennas Propag.*, vol. 68, no. 6, pp. 4172–4185, Jun. 2020.
- [35] S. Rezaee, M. Memarian, and G. V. Eleftheriades, "Dirac leaky wave antenna for millimetre-wave applications," *IET Microw., Antennas Propag.*, vol. 14, no. 9, pp. 874–883, Jul. 2020.
- [36] Y. Lin, Y. Zhang, H. Liu, Y. Zhang, E. Forsberg, and S. He, "A simple high-gain millimeter-wave leaky-wave slot antenna based on a bent corrugated SIW," *IEEE Access*, vol. 8, pp. 91999–92006, 2020.
- [37] S. K. Podilchak, A. P. Freundorfer, and Y. M. M. Antar, "Broadside radiation from a planar 2-D leaky-wave antenna by practical surface-wave launching," *IEEE Antennas Wireless Propag. Lett.*, vol. 7, pp. 517–520, 2008.
- [38] D. Comite, W. Fuscaldo, S. K. Podilchak, P. D. H. Re, V. G. Buendía, P. Burghignoli, P. Baccarelli, and A. Galli, "Radially periodic leaky-wave antenna for Bessel beam generation over a wide-frequency range," *IEEE Trans. Antennas Propag.*, vol. 66, no. 6, pp. 2828–2843, Jun. 2018.

- [39] K. Sarabandi, A. Jam, M. Vahidpour, and J. East, "A novel frequency beam-steering antenna array for submillimeter-wave applications," *IEEE Trans. THz Sci. Technol.*, vol. 8, no. 6, pp. 654–665, Nov. 2018.
- [40] Y. You, Y. Lu, Q. You, Y. Wang, J. Huang, and M. J. Lancaster, "Millimeter-wave high-gain frequency-scanned antenna based on waveguide continuous transverse stubs," *IEEE Trans. Antennas Propag.*, vol. 66, no. 11, pp. 6370–6375, Nov. 2018.
- [41] H. A. Malhat, A. S. Elhenawy, S. H. Zainud-Deen, and N. A. Al-Shalaby, "Planar reconfigurable plasma leaky-wave antenna with electronic beam-scanning for MIMO applications," *Wireless Pers. Commun.*, vol. 128, pp. 665–682, Sep. 2023.



ABDULLAH ATTAR (Student Member, IEEE) received the B.Sc. degree in applied electrical engineering from the King Fahd University of Petroleum and Minerals, Dhahran, Saudi Arabia, in 2005, and the M.Sc. degree in electrical and computer engineering from Concordia University, Montreal, QC, Canada, in 2012. His research interest includes millimeter-wave antennas.



ISLAM AFIFI (Member, IEEE) received the B.Sc. degree in electronics and communication engineering and the M.Sc. degree in engineering physics from Cairo University, Cairo, Egypt, in 2009 and 2014, respectively, and the Ph.D. degree in electrical and computer engineering from Concordia University, Montreal, QC, Canada, in 2020. He is currently a Lecturer and a Researcher with the Engineering Mathematics and Physics Department. His research interest includes millimeter-wave microwave components and antennas.



ABDEL RAZIK SEBAK (Life Fellow, IEEE) received the B.Sc. degree (Hons.) in electrical engineering from Cairo University, Cairo, Egypt, in 1976, the B.Sc. degree in applied mathematics from Ain Shams University, Cairo, in 1978, and the M.Eng. and Ph.D. degrees in electrical engineering from the University of Manitoba, Winnipeg, MB, Canada, in 1982 and 1984, respectively. From 1984 to 1986, he was with Canadian Marconi Company involving in the design of microstrip phased array antennas. From 1987 to 2002, he was a Professor with the Department of Electronics and Communication Engineering, University of Manitoba. He is currently a Professor with the Department of Electrical and Computer Engineering, Concordia University, Montreal, QC, Canada. His research interests include phased array antennas, millimeter-wave antennas and imaging, computational electromagnetics, and the interaction of EM waves with engineered materials and bio electromagnetics. He is a member of the Canadian National Committee of International Union of Radio Science Commission B. He was a recipient of the 2000 and 1992 University of Manitoba Merit Award for Outstanding Teaching and Research, the 1994 Rh Award for Outstanding Contributions to Scholarship and Research, and the 1996 Faculty of Engineering Superior. He has served as the Chair of the IEEE Canada Awards and Recognition Committee, from 2002 to 2004, and the Technical Program Chair of the 2002 IEEE CCECE Conference and the 2006 URSIANTEM Symposium. He is the Technical Program Co-Chair for the 2015 IEEE ICUWB Conference.

...